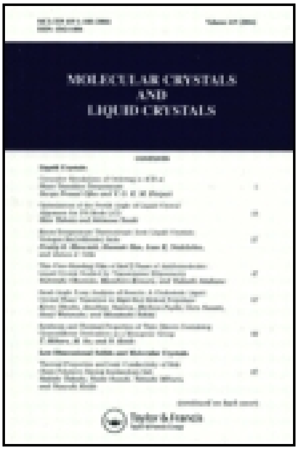

Molecular Crystals and Liquid Crystals
Publication details, including instructions for authors and subscription information:
http://www.tandfonline.com/loi/gmcl20

A Comparative Study of Charge Mobility Measurements in a Diamine and in a Hexaazatrinaphthylene Using Different Techniques

Benoit Domercq [a], Junsheng Yu [a], Bilal R. Kaafarani* [b], Takeshi Kondo [b], Seunghyup Yoo [a], Joshua N. Haddock [a], Stephen Barlow [b], Seth R. Marder [b] & Bernard Kippelen [a]

[a] Center for Organic and Photonics Electronics (COPE) School of Electrical and Computer Engineering, Georgia Institute of Technology, Atlanta, Georgia, USA

[b] Center for Organic and Photonics Electronics (COPE) School of Chemistry and Biochemistry, School of Chemistry and Biochemistry, Georgia Institute of Technology, Atlanta, Georgia, USA

Version of record first published: 22 Sep 2010

To cite this article: Benoit Domercq, Junsheng Yu, Bilal R. Kaafarani*, Takeshi Kondo, Seunghyup Yoo, Joshua N. Haddock, Stephen Barlow, Seth R. Marder & Bernard Kippelen (2008): A Comparative Study of Charge Mobility Measurements in a Diamine and in a Hexaazatrinaphthylene Using Different Techniques, Molecular Crystals and Liquid Crystals, 481:1, 80-93

To link to this article: http://dx.doi.org/10.1080/15421400701834120

Mol. Cryst. Liq. Cryst., Vol. 481, pp. 80–93, 2008
Copyright © Taylor & Francis Group, LLC
ISSN: 1542-1406 print/1563-5287 online
DOI: 10.1080/15421400701834120

A Comparative Study of Charge Mobility Measurements in a Diamine and in a Hexaazatrinaphthylene Using Different Techniques

Benoit Domercq[1], Junsheng Yu[1], Bilal R. Kaafarani[2,*], Takeshi Kondo[2], Seunghyup Yoo[1], Joshua N. Haddock[1], Stephen Barlow[2], Seth R. Marder[2], and Bernard Kippelen[1]
[1]Center for Organic and Photonics Electronics (COPE)
School of Electrical and Computer Engineering,
Georgia Institute of Technology, Atlanta, Georgia, USA
[2]Center for Organic and Photonics Electronics (COPE)
School of Chemistry and Biochemistry, School of Chemistry and Biochemistry, Georgia Institute of Technology, Atlanta, Georgia, USA

A comparative study of hole-mobility in N,N′-diphenyl-N,N′-di(3-methylphenyl)-(1,1′-biphenyl)-4,4′-diamine (TPD) using three independent measurement techniques is presented. Time-of-flight (TOF), steady-state space charge-limited current (SCLC) experiments are carried-out in neat films of TPD, sandwiched between electrodes with different work functions. Organic field-effect transistors (OFET) are fabricated from TPD thin films and their electrical properties characterized. The comparative results show that all-electrical measurements that involve carrier injection from a metal electrode into the organic film yield effective mobility values that are one order of magnitude lower than those obtained from time-of-flight experiments in which carriers are created in the film optically. Similarly, SCLC and TOF experiments were used to measure electron-mobility in a discoid organic compound 2,3,8,9,14,15-hexakis-dodecylsulfanyl-5,6,11,12,17,18-hexaazatrinaphthylene (HATNA-($SC_{12}H_{25})_6$).

Keywords: electron transport, hole-transport, liquid crystal, mobility, OFET, organic semiconductors, space charge-limited current, time-of-flight, transport

This material is based upon work supported in part by the National Science Foundation, under the STC Program (Agreement Number DMR-0120967), under the NIRT Program (DMR-0454533), and through grant CHE-0211419, by the Office of Naval Research (N00014-04-1-0120), and by Lintec Corporation.

*Current Address: Department of Chemistry, American University of Beirut, Lebanon.

Address correspondence to Bernard Kippelen, Center for Organic and Photonics Electronics (COPE), School of Electrical & Computer Engineering, Georgia Institute of Technology, 777 Atlantic Drive NW, Atlanta, GA 30332, USA. E-mail: kippelen@ece.gatech.edu

INTRODUCTION

Organic semiconductors are being used in an increasing number of optoelectronic devices and new materials will play a central role in the promising development of organic electronic technologies. An important property for these materials is charge mobility. Charge transport properties in organic semiconductors have been studied using different techniques and experimental geometries, including using the time-of-flight (TOF) method [1–4], the pulse-radiolysis time-resolved microwave conductivity (PR-TRMC) technique [5,6], the transient and steady-state space charge-limited current (SCLC) method [7–12], or using a field-effect transistor geometry (OFET) [13–15]. Among these techniques, TOF measurements have been widely used to measure charge mobility, in part because of the simplicity of the approximations that are made in analyzing the experimental data. In these experiments, widely used to characterize amorphous organic semiconductors such as polymers and molecularly-doped polymer systems, a short pulse of light generates a low density of free carriers near a transparent or semi-transparent electrode. These carriers then move in a uniform electric field across the film until they reach the opposite electrode, producing a transient current in the external circuit connected to the sample. Assuming that the material is trap-free and that the carriers move across the sample of thickness d with a constant velocity (given by μE), the measurement of the duration of that transient current allows for the determination of the mobility. Other conditions for applying this technique successfully include the following. (i) The sample must have low conductivity and electrical contacts must be non-injecting such that a uniform field can be produced. In other words, the sample without illumination must acts like a parallel plate capacitor. (ii) The geometry of the sample under such conditions must be such that the product of its resistance R and capacitance C is sufficiently small that the transient current produced by the drift of the optically created carriers in the sample occurs over a longer timescale than the RC time constant of the circuit. This condition can make it challenging to measure high mobility values in thin samples. (iii) Samples should be processed in thicknesses that are significantly larger than the optical absorption length of the short pulse.

In PR-TRMC experiments, high-intensity electron pulses (ns) produced by an accelerator irradiate the organic semiconductor and lead to the transient formation of electron-hole pairs through ionization. Mobile carriers give rise to a change in conductivity in the sample at microwave frequencies. From these changes in conductivity, the sum of hole and electron mobilities can be deduced after making several assumptions about the number of free carriers produced and yields of geminate recombination. Furthermore, one should note that the mobility values obtained using this technique can be considered intrinsic, reflecting trap-free transport in organized domains within the material or even on isolated polymer chains in dilute solutions.

In steady-state SCLC experiments, charge mobility is derived from the current-voltage characteristics of thin organic films between injecting electrodes. This method has been widely used in the past [16–19], and was applied recently by us to the characterization of electron mobility in amorphous materials [20] and columnar discotic materials [21,22]. In these experiments, the current-voltage characteristic is comprised of a linear region at low voltage and a nearly quadratic nonlinear region at high voltage that is referred to as the SCLC regime. While the current in linear region depends simultaneously on two unknown parameters – the volume density of free charges and the charge mobility – the current in the SCLC region depends only on the charge mobility and the dielectric properties and geometry of the sample. Hence, the measurement of the current values in this regime allows for the determination of the mobility. The major condition required in order to apply this technique is that one can reach this SCLC regime in a given sample geometry. Studies of carrier injection from metals into insulators have shown that such a regime is likely to be observed when the metal electrode facilitates the direct injection of excess charge into solids that have a relatively low volume density of free charges. Undoped organic semiconductors sandwiched between injecting electrodes are, therefore, good candidates. An important approximation in the analysis of these experiments is that the contact is ohmic. In practice, ideal ohmic contacts are very difficult to achieve, and the carrier injection efficiency is, therefore, seldom unity. As a result, the mobility value that can be extracted from the current measurements in the SCLC regime is an effective mobility μ_{eff} given by the product of the intrinsic mobility μ and the injection efficiency θ. Since $\theta < 1$, the effective mobility values derived from these experiments generally yield underestimates of the intrinsic mobility. As in TOF experiments, complexities can arise if the material contains traps, and, therefore, SCLC measurements give the best results in trap-free samples or in samples with shallow traps.

One limitation of the SCLC technique compared to TOF is that both holes and electrons can be injected from the appropriate electrodes and contribute to the SCLC current. The relative contribution of hole and electron conductivities can be elucidated by a careful choice of metal electrode work functions, or by characterizing organic field-effect transistors with a channel comprised of the same organic semiconductor, and source and drain electrodes fabricated from the same metals used in the SCLC measurement. For hole mobility measurements, metals should be selected such that their work function matches the energy of the highest occupied molecular orbital (HOMO) of the organic semiconductor, whereas for determining electron mobilities the lowest unoccupied molecular orbital (LUMO) energy should be matched.

In OFET experiments, charge mobility is derived from the current-voltage characteristics of the device in which current in the semiconductor flows between a source (S) and a drain (D) electrode near the interface that the semiconductor forms with an insulating gate dielectric. The current between the source and drain electrodes (I_{DS}) is controlled by applying a potential V_{GS} between the source and a gate (G) electrode. For a given value of V_{GS}, the current-voltage characteristic (I_{DS} vs. V_{DS}) exhibits a linear region followed by a saturation regime where the current is nearly constant and independent of V_{DS}. In this saturation regime, the current I_{DS} can be approximated by:

$$I_{DS} = \mu \frac{CW}{2L}(V_{GS} - V_T)^2 \tag{1}$$

where μ is the field-effect mobility, C is the capacitance density of the gate dielectric (F/cm^2), V_T is the threshold voltage, and W (width) and L (length) are the dimensions of the semiconductor channel between the source and drain electrodes. The carrier mobility in these experiments can then be derived from the measurement of the saturation current as a function of V_{GS}.

As in SCLC experiments, the mobility value extracted from these OFET experiments can be influenced by the nature of the contact between the source and drain electrodes and the semiconductor. Resistance at these contacts can influence the analysis of the data. Furthermore, charges flow in a confined region between the semiconductor and the gate dielectric and their transport can be influenced by the properties of this interface and by its topology.

Since the sample geometries and the nature of the contacts between electrodes and the semiconductor vary significantly in these different mobility measurement techniques, it can be challenging to measure charge mobility in a given compound with independent techniques. Limitations can be imposed by the processing of the organic materials into films with various thicknesses to comply with the geometry imposed by a measurement technique. One measurement technique can be easier to implement than another depending on the relative energies of the frontier orbitals (HOMO and LUMO) of the semiconductor and the workfunction of the electrode materials. Therefore, it is desirable to evaluate the differences that can arise from mobility measurements using these different techniques.

In this work, we present a comparative study of charge mobility measurements in the well known hole-transport material *N,N′*-diphenyl-*N,N′*-di(3-methylphenyl)-(1,1′-biphenyl)-4,4′-diamine (TPD) by performing both TOF and SCLC experiments in thick samples, and by characterizing a *p*-channel OFET fabricated with the same molecule. In a second part, we present the results of SCLC and TOF experiments on an discoid molecule 2,3,8,9,14,15-hexakis-dodecylsulfanyl-5,6,11,12,17,18-hexaazatrinaphthylene (HATNA-$(SC_{12}H_{25})_6$) that forms a discotic columnar liquid-crystal phase at high temperatures, but appears to retain a columnar structure in the solid state at room temperature [23–25].

Device fabrication and testing. TPD was purchased from Aldrich and purified by gradient zone sublimation prior to use. TOF samples have been prepared as described previously by sandwiching TPD films betweens electrodes with different work functions (Au and ITO) [26]. TOF and SCLC experiments have been carried out in samples with identical geometry. The active area of each device was $0.05\,cm^2$. HATNA-$(SC_{12}H_{25})_6$ was synthesized as previously described [23]. HATNA-$(SC_{12}H_{25})_6$ forms a columnar liquid crystal mesophase above 100°C. Although previous work suggests decomposition at ca. 250°C [23], we were able to heat this compound to higher temperatures without apparent decomposition and observed a second transition at 268°C that may correspond to melting to an isotropic liquid. On cooling from the liquid crystal phase it forms a mesophase of higher three dimensional order [23]. Samples for SCLC and TOF experiments were prepared by heating HATNA-$(SC_{12}H_{25})_6$ in air to 290°C on a hot plate between ITO electrodes and by letting the sample cool down to room temperature over a period of two hours in a liquid crystal hot stage. Finally, the edges of the samples were sealed with epoxy glue. The active area of each device was $0.16\,cm^2$. For SCLC experiments, the measurements of *J-V* characteristics of all devices were performed in air and in the dark. The *J-V* characteristics have been measured using a Keithley 2400 Source Meter. Capacitance was measured using an Agilent 16048 A Test Leads connected to a Agilent 4284 A Precision LCR Meter, yielding values of 4-pF for TPD and ranging from 75 to 480 pF, depending on the device thickness, for HATNA-$(SC_{12}H_{25})_6$. Transistors were fabricated as described elsewhere [27] on heavily n-doped silicon substrates with 200 nm of thermally grown silicon dioxide as the gate dielectric. Bottom contact geometry Ti/Au (10 nm/100 nm) source and drain electrodes defining channels with 500 μm and 1000 μm widths and lengths ranging from 1 μm to 50 μm were patterned on the SiO_2 layer using lift-off photolithography. Depositions were performed at room temperature using physical vapor deposition at a pressure of 5×10^{-8} Torr. The typical TPD layer thickness was 40 nm. During testing electrical connections were made with a micro-probe station contained within the second glove box and an Agilent E5272 A medium power source/monitor unit, connected to the probe station, was used to perform the electrical measurements. At no point during fabrication and testing were the transistor devices exposed to air.

Theory of steady-state SCLC with field-dependent mobility. As discussed above, SCLC regime can be attained in insulating materials when injection barrier from a metal contact is negligible. When the mobility of a material, μ, is independent of the electric field, the current density, J, in this regime is described by the Mott-Gurney law:

$$J = \frac{9}{8}\varepsilon_0\varepsilon_r\mu\frac{V^2}{d^3} \tag{2}$$

where d is the thickness of the film, V is the applied voltage, ε_0 is the permittivity of free space and ε_r is the dielectric constant of the organic semiconductor. Here, traps in the solid are ignored and charge injection efficiency is considered unity. Transport in numerous organic materials and in particular in TPD, is known to be field dependent with a general functional dependence in electric field of the form [28]:

$$\mu = \mu_0 \exp(\gamma\sqrt{E}) \tag{3}$$

where μ_0 is zero-field mobility and γ is an electric field coefficient. In this case, the derivation of the current-voltage equation is more complex. Fortunately, it has similarities with the theory of space-charge limited currents controlled by shallow traps whose effective depth is reduced by the electric field, an effect referred to as the Frenkel effect. Within this theory, the following expression of the space-charge limited current voltage characteristic was derived by Murgatroyd [29]:

$$J = \frac{9}{8}\varepsilon_0\varepsilon_r\mu_0 \exp\left(0.891\gamma\sqrt{\frac{V}{d}}\right)\frac{V^2}{d^3} \tag{4}$$

For typical values of electric-field coefficients γ established by experiments in many organic materials (10^{-2} – 10^{-4} $(\mathrm{cm/Vs})^{1/2}$), the current-voltage characteristic in the space-charge limited regime is nearly quadratic with exponents slightly larger than 2. In that nearly quadratic regime, a best fit to the data using Eq. (4) provides numerical values for μ_0 and γ. With these parameters, the effective mobility is calculated using Eq. (3). If the charge injection efficiency at the electrodes is not unity and/or if traps are present, the effective mobility that is derived from this analysis is $\mu_{eff} = \theta\mu$, with $\theta < 1$. Therefore, the mobility is an underestimation of the bulk mobility that would exist under trap-free conditions.

RESULTS AND DISCUSSION

Comparative study of hole-mobility measurements using three different techniques. TOF measurements were performed on a sample with the following geometry ITO/TPD ($d = 20\,\mu$m)/Au. Figure 1a shows typical transient photocurrents at room temperature as a function of applied field. Transient photocurrents were non-dispersive and the transient time t_t was determined directly from the linear plot of these transient photocurrents. The hole drift mobility was calculated from the transit time t_t according to the equation $\mu = d^2/V\ t_t$, where d is the sample thickness and V the applied field. Figure 1b shows that the field-dependence of the mobility is consistent with Eq. (3) with values of several times $10^{-3}\,\text{cm}^2/\text{V.s}$. These mobility values are consistent with the values published previously in the literature [30].

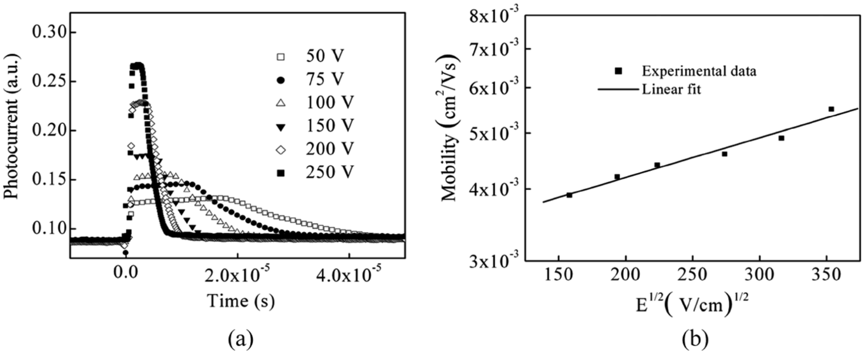

FIGURE 1 (a) Transient photocurrents for different applied field observed and (b) Electric-field dependence of the hole mobilities measured for ITO/TPD ($d = 20\,\mu$m)/Au device. Symbols represent the TOF experimental data.

SCLC measurements on a 20 μm-thick sample of TPD sandwiched between ITO and Au electrodes are shown in Figure 2. When ITO is used as the injecting contact for holes, the current density shows a linear dependence on V at low voltage. As V increases, the current density becomes a quadratic function of V, characteristic of a SCLC regime. The extracted mobility at an applied voltage of 180 V is $1.6 \times 10^{-6}\,\mathrm{cm^2/Vs}$. Under reverse bias, Au becomes the injecting electrode for holes, and the current exhibits a similar SCLC behavior but the current have higher values. That increase can be anticipated if one considers that Au has a higher work function (5.1 eV) compared with ITO (4.6–4.8 eV) and is, therefore, expected to form a better injecting contact with TPD (HOMO energy estimated at 5.3 eV). Consequently, the effective mobility extracted from the SCLC regime is two orders of magnitude higher with a value of $1.6 \times 10^{-4}\,\mathrm{cm^2/Vs}$ at 180 V. However, this value is still one order of magnitude lower than that measured in TOF experiments and can be attributed to limited injection efficiency [31].

The threshold voltage V_T at which the power dependence of the current on voltage changes from linear to quadratic is given by:

$$V_T = \frac{8}{9} e n_{fb} \frac{d^2}{\varepsilon \varepsilon_0} \tag{5}$$

where n_{fb} is the density of background free charges and e the elementary charge.

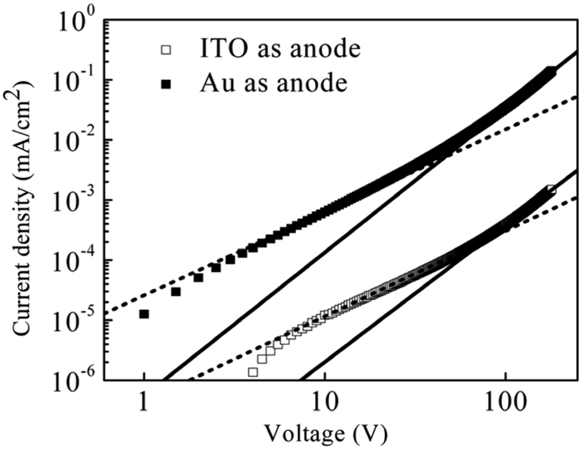

FIGURE 2 Current density-voltage characteristics for a device ITO/TPD ($d = 20\,\mu$m)/Au where ITO and Au are used successively as anode.

This expression is found by equating the expression of the current given by Ohm's law ($J \propto V$) and the Mott-Gurney expression ($J \propto V^2$). Note that the threshold voltage is independent of the carrier mobility but depends on n_{fb} and the sample geometry. Threshold voltages can be calculated using Eq. (5) by extracting first the carrier density from the linear regime of the current-density with the knowledge of the mobility values extracted from the SCLC regime. Calculated values of the threshold voltage are 72 and 48 V in positive (ITO injecting electrode) and negative bias (Au injecting electrode), respectively. These values are in good agreement with experimental values of 76 and 46 V, as shown in Figure 2.

Current-voltage and transfer characteristics of an OFET device with channel width of 500 µm, and length of 50 µm are shown in Figure 3. For the current-voltage characteristics shown in Figure 3a, the gate-source voltage V_{GS} was increased from 0 to 60 V in 5 V steps. When operated as p-channel transistors, characteristic saturation behavior was observed. Under positive gate bias, the transistors did not operate in n-channel mode, indicating that injection of holes from Au electrodes into TPD is the main origin of the current densities measured in the SCLC measurements described above. Using Eq. (1) an effective mobility value of $1.2 \times 10^{-4}\,\text{cm}^2/\text{Vs}$ was calculated from the transfer characteristic shown in Figure 3b. The linear fit to the $\sqrt{I_{DS}}$ *vs.* V_{GS} data yielded a threshold voltage of approximately -23.3 V and semi-logarithmic plots of I_{DS} *vs.* V_{GS} yielded an on/off current ratio $> 10^3$ and a sub-threshold slope of 10 Volts/decade. Mobility values were found to generally decrease with shorter channel length with typical values $2.0 \times 10^{-5}\,\text{cm}^2/\text{Vs}$ in devices with channel width of 1000 µm and length of 1 µm. The non-ohmic behavior of the current-voltage characteristics shown in Figure 3a at low V_{DS} suggests the presence of contact resistance at the source and drain electrodes. This is consistent with our attribution of the discrepancy in mobility values from TOF and SCLC measurements to limited injection efficiency. It should be noted that the hole mobility values extracted from the OFET and SCLC measurements are comparable.

Electron-mobility measurements in a hexaazatrinaphthylene using TOF and SCLC experiments. TOF measurement were performed on a sample with the following geometry: ITO/HATNA-$(SC_{12}H_{25})_6$ ($d = 104$ µm)/ITO. Figure 4a shows typical transient photocurrents at room temperature as a function of applied field. In this material, transient photocurrents were dispersive and the transient time t_t was determined using a log-log plot of these transient photocurrents. Figure 4b shows that the field-dependence of the mobility is consistent

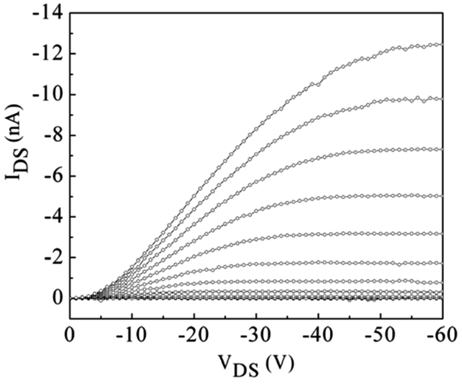

(a)

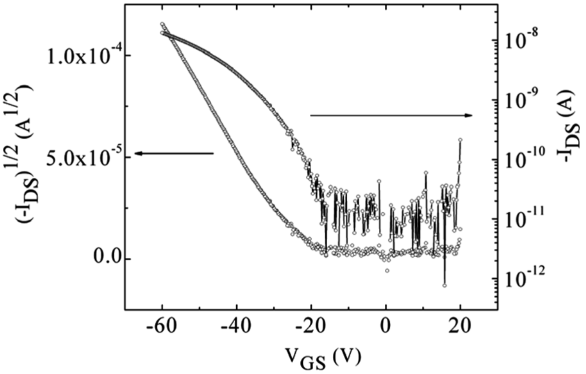

(b)

FIGURE 3 (a) Current-voltage characteristics (I_{DS} vs. V_{DS}) at several values of the gate voltage (V_{GS}) and (b) Transfer characteristics (I_{DS} and $\sqrt{I_{DS}}$ vs. V_{GS}) for a bottom contact device with $W = 500\,\mu\text{m}$, $L = 50\,\mu\text{m}$ and 40 nm of TPD.

with Eq. (3) with values of several times $10^{-3}\,\text{cm}^2/\text{Vs}$. SCLC measurements on a 10 μm-thick sample of HATNA-$(SC_{12}H_{25})_6$ sandwiched between ITO electrodes are shown in Figure 5. As shown above for TPD, the current density shows a linear dependence on V at low voltage. As V increases, the current density becomes a quadratic function of V, characteristic of a SCLC regime. The extracted mobility at a maximum applied voltage of 18 V is $1.7 \times 10^{-3}\,\text{cm}^2/\text{Vs}$. Using Eq. (5), we calculated the threshold voltage to be 12.2 V which is comparable to the experimental value of 10.7 V. The inset of Figure 5 shows the product of the current density with the film thickness ($J \times d$) as a function of the applied field (V/d) for devices with geometry

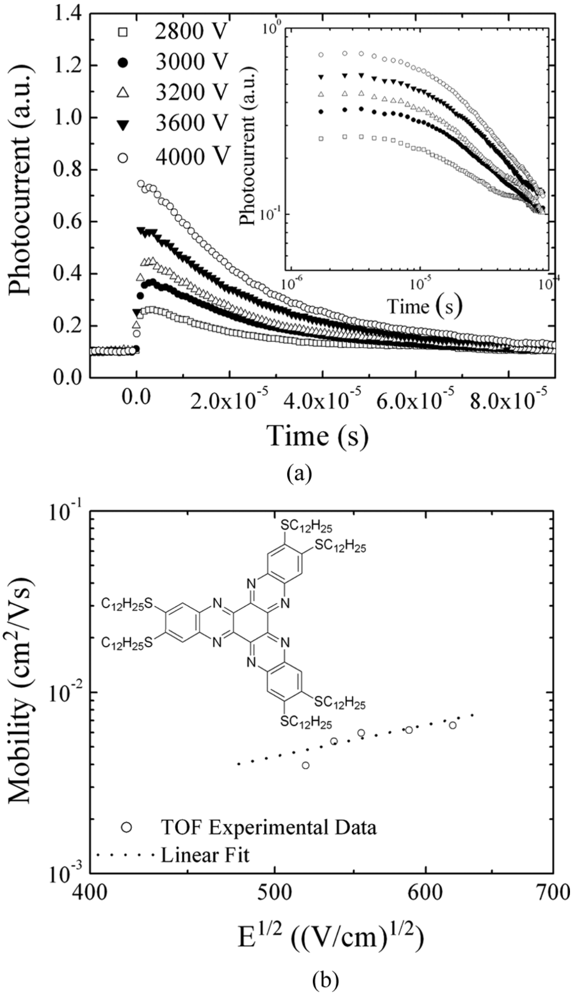

FIGURE 4 (a) Transient photocurrents measured for different applied fields (inset log-log plot of the photocurrent) and (b) Electric-field dependence of the electron mobilities measured for ITO/HATNA-$(SC_{12}H_{25})_6$ ($d = 104\,\mu m$)/ITO device. Symbols represent the TOF experimental data (inset: chemical structure of HATNA-$(SC_{12}H_{25})_6$).

ITO/HATNA-$(SC_{12}H_{25})_6$/ITO and with different thicknesses ($d = 1, 5, 10\,\mu m$). This product ($J \times d$) is independent of the thickness of the sample, as predicted by Eq. (4).

The values of the mobility determined by SCLC measurements are slightly lower than those measured by TOF but in agreement within

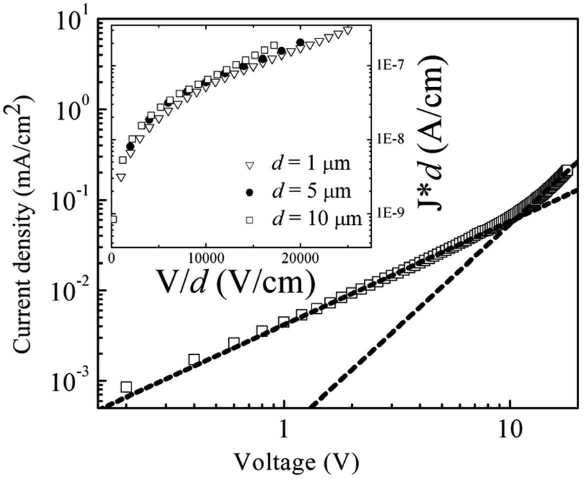

FIGURE 5 Current density-voltage characteristics for a device ITO/HATNA-$(SC_{12}H_{25})_6$ ($d = 10\,\mu m$)/ITO (inset Current-density as a function of applied field for devices ITO/HATNA-$(SC_{12}H_{25})_6$ ($d = 1, 5, 10\,\mu m$)/ITO).

a factor of two. Electron injection is probably limited by the ITO electrodes and devices using lower function metal such as silver and aluminum are currently being studied to increase electron injection efficiency. Indeed, using ITO it is possible that both holes and electrons contribute to the SCLC current (solid-state HOMO and LUMO energies of 6.0 ± 0.1 and 2.7 ± 0.4 eV have been measured for a closely analogous compound using photoelectron and inverse-photoelectron spectroscopy, respectively [32]). It is interesting to point out that PR-TRMC measurements previously made on this compound, cooled to room temperature from the liquid crystal phase, yield one-dimensional intracolumn mobilities of $0.04\,cm^2/Vs$ [26]. As mentioned in the introduction, this value can be higher than the TOF value because mobility values measured in these experiments represent the sum of hole and electron mobilities. Moreover, the intracolumn mobility is likely to be much larger than that perpendicular to the columns and so mobilities of this magnitude would be achievable in TOF or SCLC measurements if all the mesophase domains were aligned so that the columns run from one electrode to the other.

CONCLUSIONS

Mobility measurements using three different methods, TOF, OFET and SCLC, on the model hole transport material, TPD, show that the three methods lead to mobility values that differ by one order of magnitude. TOF experiments lead to the highest mobility value whereas OFET and SCLC mobility value yield consistent values that are both one order of magnitude lower. This discrepancy can be attributed to limited carrier injection efficiency between the metal electrodes and the organic material in both SCLC and OFET experiments. Similarly, mobility measurements using TOF and SCLC on an electron-transport discoid compound, HATNA-$(SC_{12}H_{25})_6$, show that mobility values are higher using TOF experiments than those using SCLC measurements. With non-amorphous materials, additional differences in mobility can be anticipated between SCLC and OFET techniques due to the difference in direction of the injected currents, namely perpendicular to the film in the case of SCLC experiments, and in the plane of the film for OFET experiments.

REFERENCES

[1] Spear, W. E. (1957). *Proc. Phys. Soc.*, *B70*, 669.
[2] Mori, T., Sugimura, E., & Mizutani T. (1993). *J. Phys. D: Appl. Phys.*, *26*, 452.
[3] Borsenberger P. M. (1990). *J. Appl. Phys.*, *68*, 5188.
[4] Borsenberger, P. M., Magin, E. H., van der Auweraer, M., & de Schryver, F. C. (1993). *Phys. Stat. Sol.*, *A140*, 9.
[5] Van de Craats, A. M. & Warman, J. M. (2001). *Adv. Mater.*, *13*, 130.
[6] Ban, K., Nishizawa, K., Ohata, K., van de Craats, A. M., Warman, J. M., Yamamoto, I., & Shirai, H. (2001). *J. Mater. Chem.*, *11*, 321.
[7] Blom, P. W. M. & de Jong, M. J. (1996). *J. J. M. Vleggaar Appl. Phys. Lett.*, *68*, 3308.
[8] Blom, P. W. M., de Jong, M. J. M., & van Munster, M. G. (1997). *Phys. Rev.*, *B55*, R656.
[9] Campbell, A. J., Bradley, D. D. C., & Lidzey, D. G. (1997). *J. Appl. Phys.*, *82*, 6326.
[10] Bozano, L., Carter, S. A., Scott, J. C., Malliaras, G. G., & Brock, P. J. (1999). *Appl. Phys. Lett.*, *74*, 1132.
[11] Shen, Y., Klein, W., Jacobs, D. B., Scott, J. C., & Malliaras, G. G. (2001). *Phys. Rev. Lett.*, *86*, 3867.
[12] Mihailetchi, V. D., van Duren, J. K. J., Blom, P. W. M., Hummelen, J. C., Janssen, R. A. J., Kroon, J. M., Rispens, M. T., Verhees, W. J. H., & Wienk, M. M. (2003). *Adv. Funct. Mater.*, *13*, 43.
[13] Dimitrakopoulos, C. D. & Mascaro, D. J. (2001). *IBM J. RES. & DEV.*, *45*, 11.
[14] Podzorov, V., Sysoev, S. E., Loginova, E., Pudalov, V. M., & Gershenson, M. E. (2003). *Appl. Phys. Lett.*, *83*, 3504.
[15] Babel, A. & Jenekhe, S. A. (2003). *J. Am. Chem. Soc.*, *125*, 13656.
[16] Abkowitz, M. & Pai, D. M. (1986). *Phil. Mag.*, *53*, 193.
[17] Poplavskyy, D. & Nelson, J. (2003) *J. Appl. Phys.*, *93*, 341.
[18] Poplavskyy, D., Nelson, J., & Bradley, D. D. C. (2003). *Appl. Phys. Lett.*, *83*, 707.
[19] de Boer, R. W. I., Jochemsen, M., Klapwijk, T. M., Morpurgo, A. F., Niemax, J., Tripathi, A. K., & Pflaum, J. (2004). *J. Appl. Phys.*, *95*, 1196.
[20] Kaafarani, B. R., Kondo, T., Yu, J., Zhang, Q., Dattilo, D., Risko, C., Jones, S. C., Barlow, S., Domercq, B., Amy, F., Kahn, A., Brédas, J.-L., Kippelen, B., & Marder, S. R. (2005). *J. Am. Chem. Soc.*, *127*, 16358.

[21] An, Z., Yu, J., Jones, S. C., Barlow, S., Domercq, B., Kippelen, B., & Marder, S. R. (2005). *Adv. Mater.*, *17*, 2580.

[22] Cho, J.-Y., Domercq, B., Yu, J., Zhang, X., Jones, S. C., An, Z., Bishop, M., Barlow, S., Marder, S. R., & Kippelen, B. (2007). *J. Mater. Chem.*, *17*, 2642.

[23] Kestemont, G., de Halleux, V., Lehmann, M., Ivanov, D. A., Watson, M. & Geerts, Y. H. (2001). *Chem. Commun.*, *20*, 2074.

[24] Roussel, O., Kestemont, G., Tant, J., de Halleux, V., Aspe, R. G., Levin, J., Remacle, A. (2003). *Mol. Cryst. Liq. Cryst.*, *396*, 35.

[25] Lehmann, M., Kestemont, G., Aspe, R. G., Buess-Herman, C., Koch, M. H. J., Debije, M. G., Piris, J., de Haas, M. P., Warman, J. M., Watson, M. D., Lemaur, V., Cornil, J., Geerts, Y. H., Gearba, R., & Ivanov, D. A. (2005). *Chem. Eur. J.*, *11*, 3349.

[26] Maldonado, J.-L., Bishop, M., Fuentes-Hernandez, C., Caron, P., Domercq, B., Zhang, Y.-D., Barlow, S., Thayumanavan, S., Malagoli, M., Brédas, J.-L., Marder, S. R., & Kippelen, B. (2003). *Chem. Mater.*, *15*, 994.

[27] Haddock, J. A., Domercq, B., & Kippelen, B. (2005). *Electronics Letters*, *41*, 444.

[28] Borsenberger, P. M., Pautmeier, L., & Bassler, H. (1991). *J. Chem. Phys.*, *94*, 5447.

[29] Murgatroyd, P. N. (1970). *J. Phys. D: Appl. Phys.*, *3*, 151.

[30] Stolka, M., Yanus, J. F., & Pai, D. M. (1984). *J. Phys. Chem.*, *84*, 4707.

[31] Shen, Y., Hosseini, A., Woi, M. H., & Malliaras, G. (2004). *Chem. Phys. Chem.*, *5*, 16.

[32] Barlow, S., Zhang, Q., Kaafarani, B. R., Risko, C., Amy, F., Chan, C. K., Domercq, B., Starikova, Z. A., Antipin, M. Y., Timofeeva, T. V., Kippelen, B., Brédas, J.-L., Kahn, A., & Marder, S. R. (2007). *Chem. Eur. J.*, *13*, 3537.